2023 European Conference on Computing in Construction
40th International CIB W78 Conference
Heraklion, Crete, Greece
July 10-12, 2023

REAL-TIME CORNER HEIGHT ESTIMATION FOR MULTI-LAYER DIRECTED ENERGY DEPOSITION USING LASER LINE SCANNER, VISION CAMERA, AND ARTIFICIAL NEURAL NETWORK

Liu Yang[1,2], Jack C.P. Cheng[1], Hoon Sohn[2], Zhanxiong Ma[2], Ikgeun Jeon[2], and Peipei Liu[2]
[1]The Hong Kong University of Science and Technology, Kowloon, Hong Kong
[2]Korea Advanced Institute of Science and Technology, Daejeon, Republic of Korea

Abstract

Metal additive manufacturing (AM) technologies, such as laser direct energy deposition (DED), have attracted attention in the construction industry. However, the current track geometry inaccuracy in the DED process, especially at corners with sharp turns, is a key barrier to the adoption of this advanced technology. To tackle geometry inaccuracy and achieve geometry control in the DED process, analytical relationships between geometry attributes and printing parameters for single-layer deposition have been developed. However, the layer height in multi-layer deposition may not be constant during the printing process, and the geometry estimation for multi-layer deposition is still problematic. Moreover, geometry estimation for corners in complex shapes has not been studied. In this study, a real-time corner height estimation technique for multi-layer track-with-corner deposition is proposed. The experimental results show that the proposed technique can estimate the corner height with an average RMSE of 0.042 mm for corners with different angles.

Introduction

Metal additive manufacturing (AM) technologies have developed rapidly since their introduction in the early 1980s because of their powerful manufacturing capability. According to the American Society for Testing and Materials (ASTM) standard, the two major groups of metal additive manufacturing technologies are directed energy deposition (DED) and powder bed fusion (PBF) (ASTM Committee, 2012), both of which have been widely applied in various fields such as the aerospace, automobile, and biomedical industries (Milewski, 2017). In recent years, DED has gained attention as a viable manufacturing method in the construction industry in which metallic materials are commonly adopted in distinctive and complex designs (Buchanan and Gardner, 2019). Traditional techniques to produce metallic components, such as hot rolling, cold forming, and extrusion, often lead to regular prismatic elements (Fröhlich and Schulenburg, 2003), which limits the potential use of metallic materials in construction and design. DED can serve as a complementary but irreplaceable technique to produce components with almost any shape with high accuracy.

However, geometry quality problems may occur during DED process especially when predefined constant printing parameters (nominal printing parameters) are used in the whole printing process. Recent studies have shown that the as-built deposition height is not always consistent with the as-designed deposition height when using constant printing parameters (Chabot et al., 2019; Tyralla et al., 2020; Vandone et al., 2018; Xiong and Zhang, 2014). This can be ascribed to three reasons. First, the value of nominal printing parameters and the corresponding as-designed track height are normally determined based on experience, which might not be accurate (Shim et al., 2016). Second, the track height is related to process parameters such as the heat emission conditions, inter layer temperatures, and surface quality of previous layers, those parameters might change at different layers (Li et al., 2021). Third, since DED process is quite sensitive to printing parameters such as laser power, powder feed rate, laser traverse speed and gas flow rate, a slight change of these parameters might lead to track height variation. Moreover, when track height deviates from as-designed value, the nozzle to top surface distance (NTSD) also deviates from specified value and the printing condition changes, result in more and more serious height discrepancy (Xiong and Zhang, 2014). In practice, if the printing system is a stable system so that the variation of printing parameters is within an acceptable range and there's no sudden disturbance on the printing parameters, most track height variations occur at discontinuities such as corner points, because the traverse speed changes at corner points (Pereira et al., 2021; Thakkar and Sahasrabudhe, 2020; Woo et al., 2019).

To ensure the performance of the final product, it is important to manage the geometry quality of deposited components. Towards geometry quality management, one important part is to identify the relationship between process parameters and geometry attributes, as illustrated in Figure 1, a proposed geometry management framework in AM process. A common AM task includes four parts, AM design, AM input, AM process and AM product. In AM design stage, product specifications such as material properties, quality characteristics and accuracy requirements, are first identified by employer, as reference for determining as-designed track geometry and toolpath. Afterwards, nominal printing parameters can be decided as AM input based on as-designed track geometry, toolpath and the relationship between printing parameters and geometry attributes. During AM process, the process parameters including real printing parameters as well as several influencing factors such as melt pool

size, interlayer temperatures, and previous layer conditions, etc., work together to produce the as-built track geometry, and finally the AM product is generated by combining all as-built tracks and thereby form the product geometry. To manage geometry quality, a control system should be considered into the common AM task, where the relationship between process parameters and track geometry attributes will be very important since it determines the prediction of control target. When there is geometry inconsistency, the nominal printing parameters can be adjusted through the established relationship to ensure the as-built track geometry.

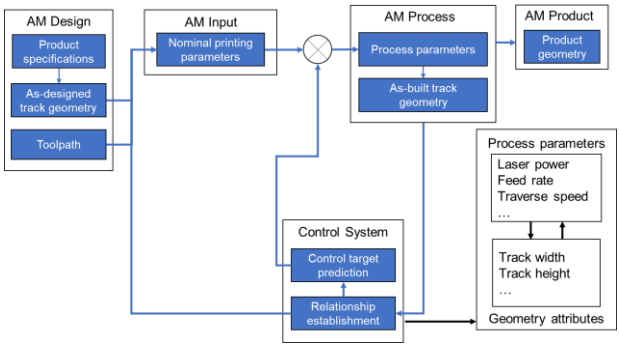

Figure 1: Geometry quality management in AM process

The relationship between geometry attributes and process parameters has been studied in previous literature. Empirical models, physics-based models together with numerical simulation, and machine learning algorithms are used to predict the track geometry from printing parameters. In early studies, the geometry estimation approaches were limited to empirical models. Afterward, to gain a better understanding of the complex laser-material interaction, physics-based models were developed. However, the physics-based models might provide worse geometry estimation accuracy compared with empirical models. Besides, numerical simulation using physics-based models takes a lot of time, making it impossible to be applied in online geometry control. Recent studies considered machine learning algorithms. Wang et al established both physics-based modeling and Gaussian Process Regression (GPR) model to predict track width and height (Wang et al., 2020). The result shows that the GPR model achieves much smaller prediction errors than physic-based modeling for track width and height, however this GPR model was established using simulated data from physic-based modeling thus the effectiveness was not validated on deposition experiments. In addition, although geometry problems often occur at corners and some studies were related to corner problems (Badarinath and Prabhu, 2021; Comminal et al., 2019; Kono et al., 2018; Ribeiro et al., 2020), there has no study focusing on the corner height estimation in DED process.

In this paper, the corner height estimation of multi-layer track-with-corner deposition has been achieved in real-time using ANN and measured traverse speed at the corner. Compared with current studies of relationship establishment methods, several machine learning algorithms have been compared and evaluated. Based on the evaluation results, an initial model for layer height estimation of multi-layer straight-track deposition using artificial neural network has been developed, considering not only three principal printing parameters (laser power, traverse speed, and powder feed rate), but also process parameters, such as layer number, previous layer height, etc. An optimal model has been constructed by updating the initial model in-situ when there has corner data with measured traverse speed been obtained. Finally, real-time corner height estimation is achieved using optimal model and measured corner speed. Through experiment, the relationship of corner height increase and corner traverse speed decrease in DED process has been quantified. Experiment results validated that the developed corner height estimation method can be applied to corners with different angles. The paper is organized as follows. Section 2 describes the experiment setup, including DED system, measurement using laser line scanner and vision camera, and the preliminary data analysis. Section 3 explains the methodology of developing real-time corner height estimation technique, which comprises offline model selection, in-situ optimal model construction and real-time corner height estimation. Sections 4 provide the experimental results and discussions. Section 5 concludes the paper by presenting summary, limitations, and future work.

Experimental setup

Description of Directed Energy Deposition System and test specimens

In this study, a commercial DED printer MX-400 from Insstek Inc. was used with 1070nm Ytterbium fiber laser system that can generate a maximum laser power of 1 kW. The powder carrier gas and shielding gas were argon gas with a flow rate of 2.5 L/min and 5.0 L/min, respectively. During deposition, the distance between nozzle and the top surface, named as nozzle to top surface distance (NTSD), should be 9 mm to achieve optimal focus of printing laser and powder distribution, and the focal laser beam diameter is 800 μm. Materials used for deposition was stainless steel 316L powder with average particle size of 100 μm and the substrate used same material with 100 mm × 50 mm × 10 mm dimension. Based on single-layer straight-track deposition trials, nominal printing parameters in the ranges of laser power between 300 and 900 W, traverse speed between 5 mm/s and 15 mm/s, and feed rate between 3 g/min and 4 g/min, were all suitable to generate layers with smooth appearance.

Two types of specimens were fabricated, multi-layer straight-track deposition and multi-layer track-with-corner deposition, including multi-layer L-shape deposition and multi-layer trapezoid-shape deposition. Specimens were manufactured under varying deposition conditions as listed in Table 1. Several different values are selected for each printing parameter within the acceptable range, and the varying deposition conditions were different combinations of nominal printing parameter

values. For multi-layer straight-track deposition, a dataset of 360 (4 × 3 × 3 × 10) samples were generated, including combinations of four laser power values of 300, 500, 700, 900 W, three traverse speed values of 5, 10, 15 mm/s, three feed rate values of 3.2, 3.6, 4 g/min and ten-layer number values. For multi-layer track-with-corner deposition, a specimen of L-shape deposition with 90-degree corner and a specimen of trapezoid-shape deposition with 45-, 90-, and 135-degree corners were manufactured.

Vision camera setup and measurement

An artificial target was attached to the nozzle, and a vision camera (SONY α6400) was installed 1 m away from the target to trace the target movement, which is the movement of nozzle (Figure 2). The camera records images and a normalized cross-correlation (NCC)-based template matching was adopted here for target tracking (Ma et al., 2020). The speed of the nozzle was calculated using the target movement between two consecutive images.

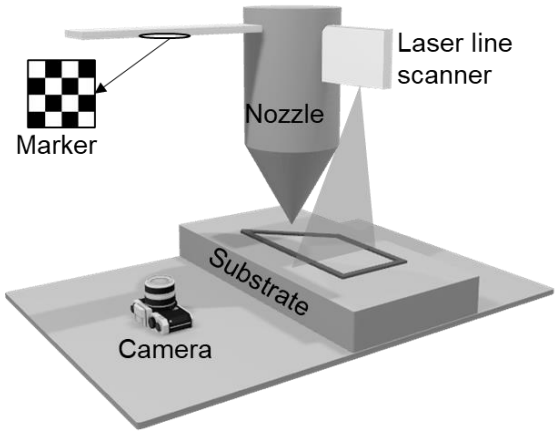

Figure 2: Experiment setup

Laser line scanner setup and measurements

To obtain geometry information of the deposited object during DED process, a laser line scanner (Micro-Epsilon scanCONTROL 3000-25/BL) was attached on the nozzle of the DED printer and move along with the nozzle during deposition. More details can be found in (Binega et al., 2022).

The laser line scanner is calibrated so that the projected laser line was perpendicular to the printing direction to capture the cross-section profiles of the deposited object. Figure 3 shows typical cross-section profiles of different specimens. For each profile, a region of interest (ROI) points is selected as the points of printed part and the position of ROI is determined through calibration. The height of each profile is defined as the average height of the ROI points within the top 90th percentile of the height values. For multi-layer straight-track deposition, the deposition height (DH) at a specific layer was the average height of profiles from this layer. For multi-layer track-with-corner deposition, the deposition height of straight part is defined same as in multi-layer straight track. While the deposition height of each corner at a specific layer was the average height of the corresponding corner profiles from this layer, and the corner profiles were profiles within 1mm distance from each corner position.

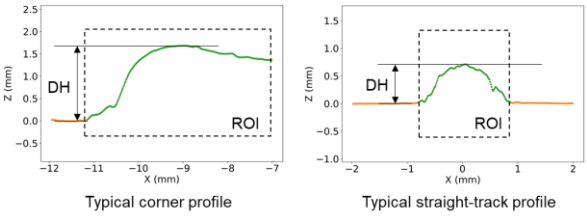

Figure 3: Typical profiles from lase line scanner

Research Methodology

Overview of proposed method

According to previous literature and experimental practice, it is common to experimentally determine the relationship between the printing parameters and the layer height before printing. Therefore, the general idea of our proposed corner height estimation technique is to make use of the relationship study from multi-layer straight-track deposition and expand its application to multi-layer track-with-corner deposition. The proposed technique for corner geometry measurement consists of three parts as shown in Figure 4. First part is offline model selection using multi-layer straight-track data, where candidates of machine learning algorithms are compared using multi-layer straight-track data with several candidates of feature combinations. An initial model is determined with selected algorithm and feature combination and used as a base model for corner height estimation. Since the data distribution of corner data is different with the data distribution of straight-track, the idea of the second part is to update the initial model when an amount of the multi-layer track-with-corner data with speed correction is obtained in-situ. Finally, an optimal model is determined, and the third part is to estimate corner height during multi-layer track-with-corner deposition in real-time.

Offline model selection

(1) Input features and output target

The output target is layer heigh, which is defined as the increment of deposition height while a new layer is deposited. For model training, the layer height as output target is obtained from laser line scanner, calculated as the difference of deposition height between neighboring layers.

The input features include laser power, traverse speed, feed rate, layer number, nozzle to top surface distance, previous deposition height and previous layer height. Since DED is a process of melting and solidifying metal powder with energy, the factors directly related to powder and energy should have large importance to track geometry. Hence, the three main printing parameters that determine track geometry are laser power, feed rate and traverse speed, proved by a lot of experiments and

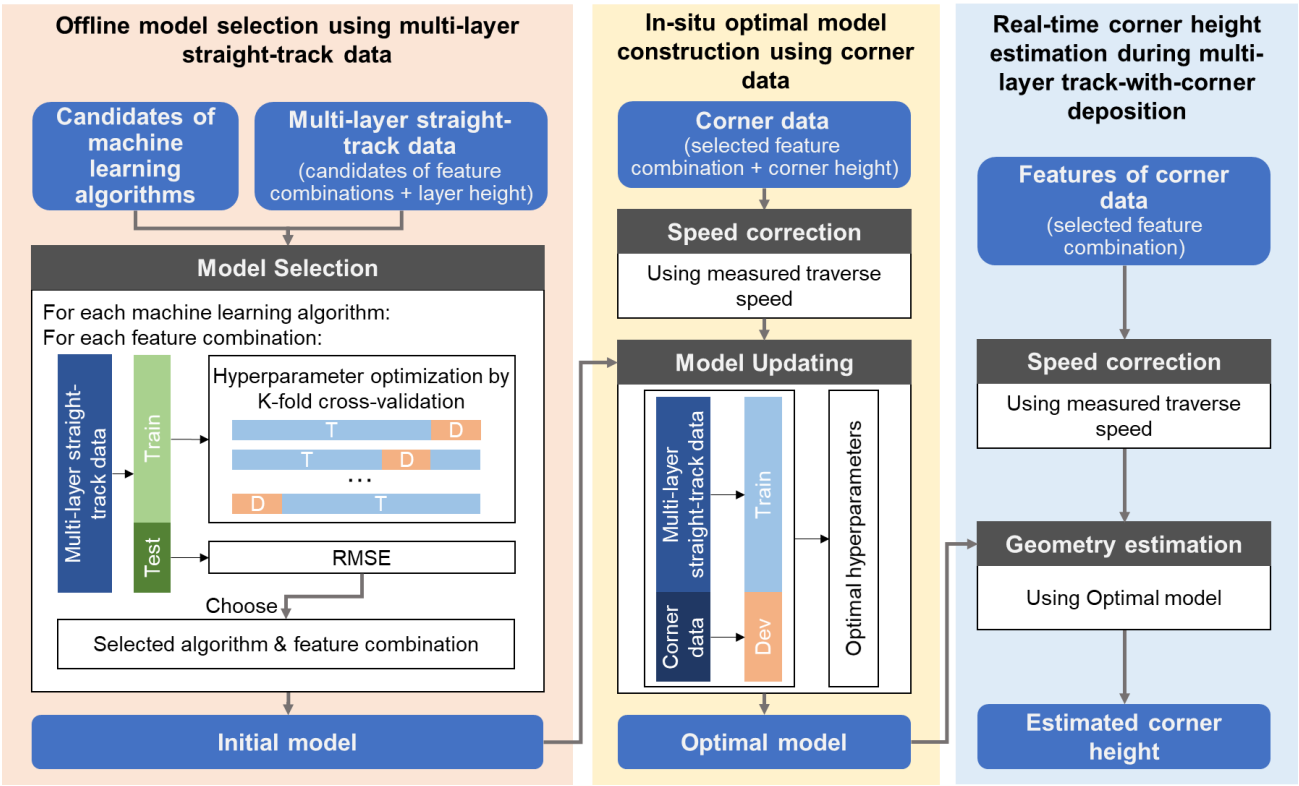

Figure 4: Overview of proposed method

numerical analysis in previous literatures (Lee and Farson, 2016). These three printing parameters are selected as input features in this study. Apart from the three main printing parameters, there are other parameters that might provide useful information in layer height estimation. A lot of studies do not consider layer number and conduct layer height estimation for single track using three main printing parameters and the results have been used for layer height control. However, the layer height might not be constant and have a trend to become smaller during multi-layer deposition since the heat cumulates as more layer deposited. Besides, nozzle to top surface distance has been proved to influence the geometry since it changes the printing conditions. Since the role of these parameters is uncertain and might be redundant for our model, feature selection is conducted. Different input feature combinations are generated and compared in the next step to select the best feature combination.

(2) Model training and evaluation

Six machine learning algorithms are trained and compared in this study, including Linear Regression, second order Multivariate Polynomial Regression (MPR), ANN, Decision Tree, Random Forest and AdaBoosting. Linear regression is the simplest and most commonly used algorithm for regression problems. The estimation model can be represented in equation (1), where $x= [x_1, x_2 \dots x_D]$ is the input features and y are the output target. Early literatures mostly adopt this approach but suffer from low estimation accuracy since the relationship between printing parameters and layer height are nonlinear. Multivariate Polynomial Regression could represent nonlinear relationship and thus adopted and compared with other algorithms. The estimation model using second order MPR is shown in equation (2).

$$y(x,w) = w_0 + w_1x_1 + \cdots + w_Dx_D \quad (1)$$

$$y(x,w) = w_0 + \sum_{k=1}^{D} w_k x_k + \sum_{i=1}^{D}\sum_{j=i}^{D} w_{ij} x_i x_j \quad (2)$$

Except traditional regression algorithms, ANN model has strong capability to approximate nonlinear relationships and has been widely used in system identification in intelligent control field (Bavarian, 1988). A typical ANN model consists of an input layer, an output layer and one or more hidden layers, each hidden layer contains several hidden neurons (Bishop, 2006). The adjustment of hyperparameters is an essential part in the training of machine learning models and significantly influences the model performance. The main hyperparameters of ANN model include number of layers, number of neurons, L2 penalty parameter, learning rate, solver, and activation function. Selection of the number of layers has been discussed in (Haykin, 2009). An ANN model with one hidden layer is capable to approximate any nonlinear relationship, but model with deeper hidden layers could have better ability to fit the function, although at the expenses of introducing overfitting problem and increasing training difficulties. Similarly, small number of neurons may lead to underfitting while too many neurons will create overfitting problem and increase training time.

Another class of algorithms for solving regression problems is the tree algorithm which is based on decision tree. Regression tree from Classification and Regression

Trees (CART) is adopted as d ecision tree algorithm in this study, in which the optimal split point is selected by least square method. The hyperparameters considered to be tuned are the maximum depth of tree (max_depth) and the minimum number of samples required to split an internal node (min_samples_split). Random forest is an algorithm based on decision tree, which uses bootstrap to select samples from dataset and randomly selects multiple features from all features to determine the best splitting point when build one CART decision tree. Several CART trees are built to form a forest and finally determine the prediction by voting. The hyperparameters considered to be tuned in our study include the two hypermeters of decision tree, maximum depth of tree (max_depth) and the minimum number of samples required to split an internal node (min_samples_split), and the number of trees in the forest (n_estimators). Adaboost is an iterative algorithm whose main idea is to train different classifiers (weak classifiers) for the same training set, and then to aggregate these weak classifiers to form a stronger final classifier (strong classifier). The hyperparameters considered to be tuned include the aforementioned two decision tree parameters and the weight applied to each classifier at each boosting iteration (learning_rate).

For each machine learning algorithm and each feature combination, the multi-layer straight-track data is divided into train set and test set. Hyperparameter optimization is conducted using the train set by k-fold cross-validation, where the train set is further divided into train and validation set. After determining the hyperparameters of each machine learning algorithm under each feature combination, the test set is used to evaluate the performance by calculating the Root Mean Square Error (RMSE) between estimated layer height and measured layer height.

In-situ construction of optimal model and Real-time corner height estimation during multi-layer track-with-corner deposition

When it comes to corner height estimation, our test data set becomes corner data. First, a speed correction should be conducted for corner data since the actual traverse speed at corner is not same as the nominal traverse speed. Second, considering the distribution of straight track data and corner track data might be different, directly applying the initial model to corner height estimation result in bad performance. Therefore, the initial model is updated when there is a batch of corner data obtained in-situ. In practice, the in-situ construction of optimal model can be conducted regularly when a certain amount of new corner data was acquired, so that the performance of our model will continue to improve.

After obtaining the optimal model, the real-time corner height estimation can be conducted. The real-time measured traverse speed is used in speed correction and the geometry estimation is conducted using optimal model.

Experiment results

Results of offline model selection

An initial model should be selected with the smallest RMSE by comparing different algorithms with different feature combinations. The three principal printing parameters are determined to be the input features while the other four process parameters are to be determined, thus there are in total 16 feature combinations considering all possible cases. Figure 5 shows the RMSE of six algorithms with representative feature combinations. For all six algorithms, considering only three principal printing parameters will give the worst estimation performance compared with considering more features. For all feature combinations, linear regression algorithm performs notably worse than the other five algorithms that can represent non-linear relationship. In addition, the best feature combination for all algorithms is hard to determine since different algorithms may achieve its best performance with different feature combinations.

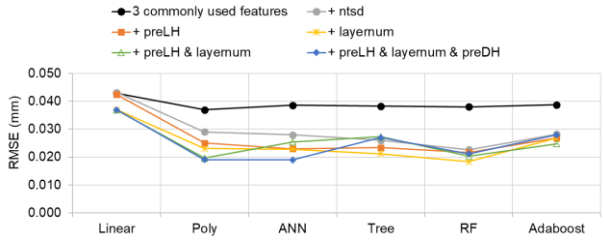

Figure 5: RMSE of layer height estimation of multi-layer straight-track deposition with different algorithms and feature combinations

Finally, the model with smallest RMSE (0.019mm) is selected as the initial model, which is ANN model with three principal printing parameters (laser power, feed rate and traverse speed) and three other parameters (preLH, layer number and preDH). Figure 6 shows the layer estimation performance of the initial model on test samples, which achieves RMSE of 0.019mm.

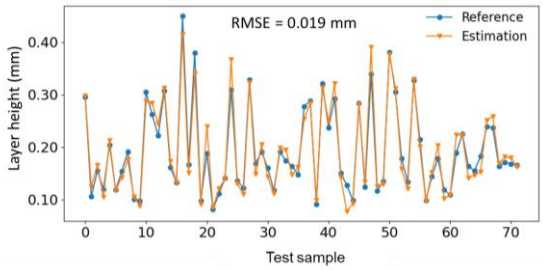

Figure 6: Layer height estimation of multi-layer straight-track deposition using optimal model

Results of in-situ construction of optimal model

The in-situ construction of optimal model is validated on 18-layer L-shape deposition. The collected data from 18-layer L-shape deposition is divided into validation set and test set. The optimal model is determined by adjusting hyperparameters of the initial model using validation set by Bayesian optimization. The performance of optimal model is validated on test set. Figure 7 (a) shows the performance of the initial model and Figure 7 (b) shows

the performance of optimal model, where the optimal model has lower RMSE.

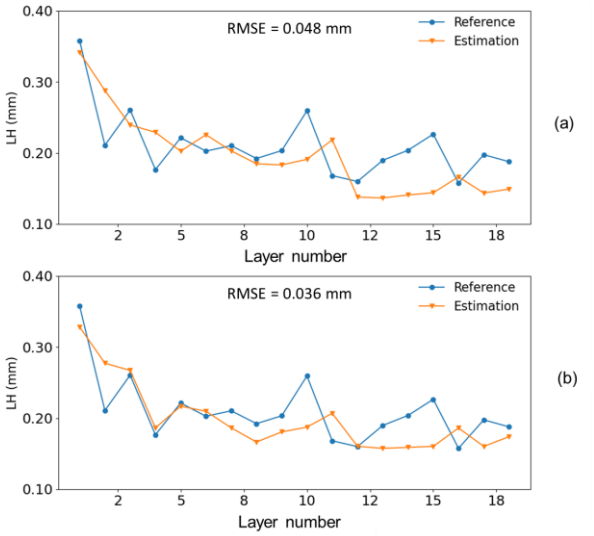

Figure 7: Example of comparing (a) Corner height estimation using initial model and (b) Corner height estimation using optimal model

Results of real-time corner height estimation results

After determining the optimal model, real-time corner height estimation has been conducted on five specimens with different printing parameters as listed in Table 1. The performance of speed correction has been validated by comparing the estimated corner height with real-time measured traverse speed and the estimated corner height with designed traverse speed at different corners. The improvement of integrating speed correction is defined in equation (3), where $RMSE_{(Vreal)}$ is the RMSE of corner height estimation using measure traverse speed and $RMSE_{(Vdesign)}$ is the RMSE of corner height estimation using as-designed traverse speed.

$$\text{Improvement} = \frac{RMSE_{(Vreal)} - RMSE_{(Vdesign)}}{\text{Average layer height}} \quad (3)$$

Table 1: Specimens for real-time corner height estimation

	Power (W)	Speed (mm/s)	Feed rate (g/min)	Number of Layer
Trapezoid-shape	1	700	10	3.6	18
	2	500	10	3.6	18
	3	600	15	4	18
	4	500	10	3.2	18
	5	700	15	3.6	18

Table 2 shows the corner height estimation results using optimal model and the improvement of integrating speed correction. As can be seen from Table 2, the improvement of speed correction was validated since $RMSE_{(Vreal)}$ is always smaller than $RMSE_{(Vdesign)}$. For corners with sharper angles, the speed decease and the layer height increase are more serious and thus the improvement of speed correction is more remarkable.

Table 2: Corner height estimation using optimal model

Trapezoid-shape		RMSE (mm)		Improvement
		Vreal	Vdesign	
Corner 135°	1	0.036	0.042	2.7%
	2	0.047	0.051	2.3%
	3	0.040	0.109	32.3%
	4	0.052	0.058	3.1%
	5	0.039	0.046	3.4%
Corner 90°	1	0.028	0.044	8.1%
	2	0.035	0.053	9.5%
	3	0.024	0.111	40.1%
	4	0.032	0.056	12.7%
	5	0.030	0.051	10.1%
Corner 45°	1	0.056	0.104	24.9%
	2	0.075	0.112	18.8%
	3	0.049	0.181	61.4%
	4	0.040	0.110	36.2%
	5	0.048	0.113	32.2%
Average RMSE		0.042		

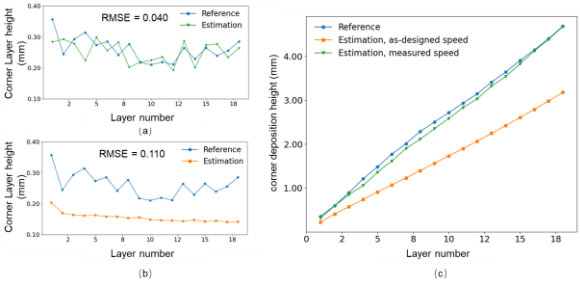

Figure 8: Example of corner height estimation of corner 45° on trapezoid-shape deposition using optimal model. (a) reference and estimated corner height with measured traverse speed, (b) reference and estimated corner height with as-designed traverse speed, and (c) reference and estimated deposition height at corner

Figure 8 shows an example of corner height estimation on trapezoid-shape deposition using the optimal model (corner 45°, sample 4). The blue line is reference height measured by laser line scanner, the orange line is the estimation using as-designed speed, and the green line is estimation using as-designed speed. It is evident that the corner layer height estimation result using measured traverse speed is much better than using as-designed speed as presented in Figure 8 (a) and (b). Furthermore, Figure 8(c) shows the estimated and reference deposition height, which is cumulation of estimated and reference layer height, respectively. It can be seen that the estimated deposition height using measured speed is quite close to the reference deposition height. This indicates that although there still has a RMSE of 0.042 mm on layer

height estimation at corner using measured speed, the error did not cumulate as more layers deposited.

Conclusions

In this study, a real-time corner height estimation technique for multi-layer track-with-corner deposition has been developed using laser line scanner, vision camera and artificial neural network. Reference layer height can be obtained using laser line scanner and traverse speed at corners can be measured by vision camera with templated matching-based computer vison algorithm. The corner traverse speed decrease and corner height increase has been observed and quantitively analyzed. An initial model has been constructed using multi-layer straight-track data by evaluating different machine learning algorithms with different feature combinations. An optimal model for corner height estimation has been constructed in-situ by updating the initial model using corner data with measured traverse speed. Real-time corner height estimation is conducted through trapezoid-shape deposition with five samples and the experimental result validated the effectiveness of our proposed technique.

There are some limitations and future work of this study. First, only three different angles (45°, 90° and 135°) are validated using the proposed method, a more general analysis of all angles should be considered in future study. Besides, this study only considered deposition using SS316L, and the adaptability of the proposed method to other materials and validation experiments might be needed.

Acknowledgments

This work was supported by the National Research Foundation of Korea (NRF) grant funded by the Korean government (MSIT) (grant number: 2019R1A3B3067987).

References

ASTM Committee, 2012. Standard terminology for additive manufacturing technologies. ASTM International.

Badarinath, R., Prabhu, V., 2021. Integration and evaluation of robotic fused filament fabrication system. Addit. Manuf. 41, 101951. https://doi.org/10.1016/j.addma.2021.101951

Bavarian, B., 1988. Introduction to neural networks for intelligent control. IEEE Control Syst. Mag. 8, 3–7.

Binega, E., Yang, L., Sohn, H., Cheng, J.C.P., 2022. Online geometry monitoring during directed energy deposition additive manufacturing using laser line scanning. Precis. Eng. 73, 104–114. https://doi.org/10.1016/j.precisioneng.2021.09.005

Bishop, C.M., 2006. Pattern recognition and machine learning, Information science and statistics. Springer, New York.

Buchanan, C., Gardner, L., 2019. Metal 3D printing in construction: A review of methods, research, applications, opportunities and challenges. Eng. Struct. 180, 332–348. https://doi.org/10.1016/j.engstruct.2018.11.045

Chabot, A., Rauch, M., Hascoët, J.-Y., 2019. Towards a multi-sensor monitoring methodology for AM metallic processes. Weld. World 63, 759–769. https://doi.org/10.1007/s40194-019-00705-4

Comminal, R., Serdeczny, M.P., Pedersen, D.B., Spangenberg, J., 2019. Motion planning and numerical simulation of material deposition at corners in extrusion additive manufacturing. Addit. Manuf. 29, 100753. https://doi.org/10.1016/j.addma.2019.06.005

Fröhlich, B., Schulenburg, S., 2003. Metal architecture: design and construction. Birkhauser.

Haykin, S.S., 2009. Neural networks and learning machines, 3rd ed. ed. Prentice Hall, New York.

Kono, D., Maruhashi, A., Yamaji, I., Oda, Y., Mori, M., 2018. Effects of cladding path on workpiece geometry and impact toughness in Directed Energy Deposition of 316L stainless steel. CIRP Ann. 67, 233–236. https://doi.org/10.1016/j.cirp.2018.04.087

Lee, Y.S., Farson, D.F., 2016. Surface tension-powered build dimension control in laser additive manufacturing process. Int. J. Adv. Manuf. Technol. 85, 1035–1044. https://doi.org/10.1007/s00170-015-7974-5

Li, G., Odum, K., Yau, C., Soshi, M., Yamazaki, K., 2021. High productivity fluence based control of Directed Energy Deposition (DED) part geometry. J. Manuf. Process. 65, 407–417. https://doi.org/10.1016/j.jmapro.2021.03.028

Ma, G., Li, Y., Wang, L., Zhang, J., Li, Z., 2020. Real-time quantification of fresh and hardened mechanical property for 3D printing material by intellectualization w

ith piezoelectric transducers. Constr. Build. Mater. 241 , 117982. https://doi.org/10.1016/j.conbuildmat.2019.1 17982

Milewski, J.O., 2017. Additive Manufacturing of Metals, Springer Series in Materials Science. Springer Interna tional Publishing, Cham. https://doi.org/10.1007/978-3 -319-58205-4

Pereira, J.C., Borovkov, H., Zubiri, F., Guerra, M.C., Ca minos, J., 2021. Optimization of Thin Walls with Shar p Corners in SS316L and IN718 Alloys Manufactured with Laser Metal Deposition. J. Manuf. Mater. Process . 5, 5. https://doi.org/10.3390/jmmp5010005

Ribeiro, K.S.B., Mariani, F.E., Coelho, R.T., 2020. A Stu dy of Different Deposition Strategies in Direct Energy Deposition (DED) Processes. Procedia Manuf. 48, 663 –670. https://doi.org/10.1016/j.promfg.2020.05.158

Shim, D.-S., Baek, G.-Y., Seo, J.-S., Shin, G.-Y., Kim, K .-P., Lee, K.-Y., 2016. Effect of layer thickness setting on deposition characteristics in direct energy depositi on (DED) process. Opt. Laser Technol. 86, 69–78. http s://doi.org/10.1016/j.optlastec.2016.07.001

Thakkar, D., Sahasrabudhe, H., 2020. Investigating micr ostructure and defects evolution in laser deposited sing le-walled Ti6Al4V structures with sharp and non-shar p features. J. Manuf. Process. 56, 928–940. https://doi. org/10.1016/j.jmapro.2020.05.052

Tyralla, D., Köhler, H., Seefeld, T., Thomy, C., Narita, R ., 2020. A multi-parameter control of track geometry a nd melt pool size for laser metal deposition. Procedia CIRP 94, 430–435. https://doi.org/10.1016/j.procir.20 20.09.159

Vandone, A., Baraldo, S., Valente, A., 2018. Multisensor Data Fusion for Additive Manufacturing Process Cont rol. IEEE Robot. Autom. Lett. 3, 3279–3284. https://d oi.org/10.1109/LRA.2018.2851792

Wang, S., Zhu, L., Fuh, J.Y.H., Zhang, H., Yan, W., 202 0. Multi-physics modeling and Gaussian process regre ssion analysis of cladding track geometry for direct en ergy deposition. Opt. Lasers Eng. 127, 105950. https:// doi.org/10.1016/j.optlaseng.2019.105950

Woo, Y.-Y., Han, S.-W., Oh, I.-Y., Moon, Y.-H., Ha, W. , 2019. Control of Directed Energy Deposition Process to Obtain Equal-Height Rectangular Corner. Int. J. Pr ecis. Eng. Manuf. 20, 2129–2139. https://doi.org/10.10 07/s12541-019-00226-6

Xiong, J., Zhang, G., 2014. Adaptive control of deposited height in GMAW-based layer additive manufacturing. J. Mater. Process. Technol. 214, 962–968. https://doi. org/10.1016/j.jmatprotec.2013.11.014